Application of numerical quantum transfer-matrix approach in the randomly diluted quantum spin chains

Ryszard Matysiak, Philipp Gegenwart, Akira Ochiai, Frank Steglich

Angaben zur Veröffentlichung / Publication details:

Matysiak, Ryszard, Philipp Gegenwart, Akira Ochiai, and Frank Steglich. 2018. "Application of numerical quantum transfer-matrix approach in the randomly diluted quantum spin chains." *Lecture Notes in Computer Science* 10778: 359–67. https://doi.org/10.1007/978-3-319-78054-2_34.

Application of Numerical Quantum Transfer-Matrix Approach in the Randomly Diluted Quantum Spin Chains

Ryszard Matysiak[1(✉)], Philipp Gegenwart[2,3], Akira Ochiai[4], and Frank Steglich[2]

[1] Institute of Engineering and Computer Education, University of Zielona Góra, ul. prof. Z. Szafrana 4, 65-516 Zielona Góra, Poland
r.matysiak@iibnp.uz.zgora.pl
[2] Max Planck Institute for Chemical Physics of Solids, 01187 Dresden, Germany
[3] Experimental Physics VI, Center for Electronic Correlations and Magnetism, University of Augsburg, 86159 Augsburg, Germany
[4] Center for Low Temperature Science, Tohoku University, Sendai 980-8578, Japan

Abstract. The description of the numerical method of simulation based on the quantum transfer-matrix (QTM) approach is presented for diluted spin $S = 1/2$ chains. Modification of the extrapolation technique has been used to obtain better accuracy of numerical results. The simulations have been performed using the $S = 1/2$ antiferromagnetic Heisenberg model with the transverse staggered field and a uniform magnetic field perpendicular to the staggered field applicable for the diluted compound $(Yb_{1-x}Lu_x)_4As_3$. In the model calculations the fixed microscopic parameters established earlier for the pure system have been assumed and the random impurity distribution has been considered. The experimental field-dependent specific heat of the polydomain diluted $(Yb_{1-x}Lu_x)_4As_3$ sample is compared with that calculated using the HPC resources and providing additional verification of both the QTM method and the physical model.

Keywords: Quantum transfer-matrix method
Segmented Heisenberg antiferromagnet · One-dimensional spin chains

1 Introduction

One-dimensional systems have attracted the interest of physicists and chemists for more then three decades. The theory of ideally uniform $S = 1/2$ antiferromagnetic Heisenberg chain in the magnetic field is well established and the properties observed in real systems are usually well described. A new class of rare-earth compounds like Yb_4As_3 have become the focus of attention. At high-temperatures ($T > 295$ K), Yb_4As_3 is a homogeneous intermediate valent (IV) metal with a cubic crystal structure. The Yb ions reside statistically on four

equivalent families of chains along the space diagonals of a cube [1]. At low-temperatures the crystal Yb_4As_3 shrinks along the $\langle 111 \rangle$ direction getting a trigonal structure and the Yb^{3+} ions form a one-dimensional spin $S = 1/2$ chain along the $\langle 111 \rangle$ direction. The remaining Yb ions occupy nonmagnetic divalent states. The neutron scattering experiments on pure Yb_4As_3 have confirmed that the excitation spectrum is well described by the one-dimensional $S = 1/2$ isotropic Heisenberg model [2] in the absence of magnetic field. The interchain interactions are small and ferromagnetic, leading to a spin-glass freezing at low temperatures [3] which are below the region analyzed for the diluted samples. The system has attracted a lot of interest due to its striking quantum properties such as the energy gap formation in the magnetic field [4] and Bose-glass effects recently observed [5].

To simulate the finite-temperature properties of the pure Yb_4As_3 and the diluted $(Yb_{1-x}Lu_x)_4As_3$ systems we consider the $S = 1/2$ anisotropic Heisenberg model with the antisymmetric Dzyaloshinskii–Moriya interaction [6,7]:

$$\mathcal{H} = -\Bigg\{ J \sum_{i=1}^{L} \left[\hat{\mathcal{S}}_i^z \hat{\mathcal{S}}_{i+1}^z + \cos(2\theta) \left(\hat{\mathcal{S}}_i^x \hat{\mathcal{S}}_{i+1}^x + \hat{\mathcal{S}}_i^y \hat{\mathcal{S}}_{i+1}^y \right) \right] + \\ + J \sin(2\theta) \sum_{i=1}^{L} (-1)^i \left(\hat{\mathcal{S}}_i^x \hat{\mathcal{S}}_{i+1}^y - \hat{\mathcal{S}}_i^y \hat{\mathcal{S}}_{i+1}^x \right) + g_\perp \mu_B B \sum_{i=1}^{L} \hat{\mathcal{S}}_i^x \Bigg\}, \qquad (1)$$

where L is the number of spins in the chain, J denotes the nearest–neighbour interaction constant, B is the external magnetic field and g is the gyromagnetic ratio.

The Dzyaloshinskii–Moriya interaction is eliminated by rotating the spins in the x–y plane by the angle θ [8]:

$$\begin{aligned} \hat{\mathcal{S}}_i^x &= \cos(\theta) \mathcal{S}_i^x + (-1)^i \sin(\theta) \mathcal{S}_i^y \\ \hat{\mathcal{S}}_i^y &= -(-1)^i \sin(\theta) \mathcal{S}_i^x + \cos(\theta) \mathcal{S}_i^y \\ \hat{\mathcal{S}}_i^z &= \mathcal{S}_i^z \end{aligned} \qquad (2)$$

Then the model is mapped onto

$$\mathcal{H} = -J \sum_{i=1}^{L} \mathbf{S}_i \mathbf{S}_{i+1} - g_\perp \mu_B B^x \sum_{i=1}^{L} S_i^x - g_\perp \mu_B B_s^y \sum_{i=1}^{L} (-1)^i S_i^y, \qquad (3)$$

where $B^x = B\cos(\theta)$, $B_s^y = B\sin(\theta)$ and B is the uniform external magnetic field perpendicular to the one–dimensional spin–chain. If the magnetic field B is applied along the spin–chain we replace $\theta = 0$ and $g_\perp = g_\parallel$.

Using hamiltonian (3) we can describe thermodynamic properties of the pure and diluted system both in the absence and the presence of external magnetic field. In the model (3) all the parameters are fixed and the values arise from the earlier studies [8–10]. The g factors for the applied field along the directions parallel and perpendicular to the spin chain amount to $g_\parallel = 3.0$ and $g_\perp = 1.3$, the exchange coupling $J/k_B = -28$ K and the transformation angle corresponds to the value $\tan(\theta) = 0.19$.

2 Description of the Model and the Simulation Technique

To characterize the finite-temperature properties of one-dimensional systems we need to calculate the free energy $\mathcal{F} = -k_B T \ln(\mathcal{Z})$ which is related to the partition function $\mathcal{Z}$ defined as:

$$\mathcal{Z} = \mathbf{Tr} e^{-\beta \mathcal{H}}, \tag{4}$$

where $\beta = 1/(k_B T)$. The values of matrix elements of $e^{-\beta \mathcal{H}}$ cannot be found exactly for large L because of noncommuting operators in $\mathcal{H}$ so we look for the systematic approximants $\mathcal{Z}_m$ to the partition function $\mathcal{Z}$, where m is the natural number (the Trotter number). In the framework of the transfer-matrix method [11,12], first we divide the Hamiltonian (3) into two noncommuting parts $\mathcal{H}^{odd}$, $\mathcal{H}^{even}$:

$$\mathcal{H} = \mathcal{H}^{odd} + \mathcal{H}^{even} = (\mathcal{H}_{1,2} + \ldots + \mathcal{H}_{L-1,L}) + (\mathcal{H}_{2,3} + \ldots + \mathcal{H}_{L,1}) \tag{5}$$

each part defined by the commuting spin-pair operators $\mathcal{H}_{i,i+1}$:

$$\mathcal{H}_{i,i+1} = -J \mathbf{S}_i \mathbf{S}_{i+1} - \frac{1}{2} g_{\perp} \mu_B \left[B^x \left(S_i^x + S_{i+1}^x \right) + (-1)^i B_s^y \left(S_i^y + S_{i+1}^y \right) \right]. \tag{6}$$

For the infinite chains in the limit $L \to \infty$ the partition function $\mathcal{Z}_m$ is equal to the highest eigenvalue [12–16] of the global transfer matrix $\mathcal{W}$ [17]:

$$Z_m = Tr \left(\mathcal{W} \right)^L, \tag{7}$$

where

$$\mathcal{W} = \prod_{r=1}^{2m} \mathcal{L}_{r,r+1} = \left(\mathcal{P} \mathcal{L}_{1,2} \right)^{2m}. \tag{8}$$

The local transfer matrix $\mathcal{L}$ whose elements depend on $\mathcal{V}$ elements is defined as:

$$\langle S_{r,i}^z S_{r+1,i}^z \mid \mathcal{L}_{r,r+1} \mid S_{r,i+1}^z S_{r+1,i+1}^z \rangle = \langle S_{r,i}^z S_{r,i+1}^z \mid \mathcal{V}_{i,i+1} \mid S_{r+1,i}^z S_{r+1,i+1}^z \rangle, \tag{9}$$

where $\mathcal{V}_{i,i+1} = e^{-\beta \mathcal{H}_{i,i+1}/m}$ and the shift operator $\mathcal{P}$:

$$\mathcal{P} \equiv \sum_{S_1^z} \ldots \sum_{S_{2m}^z} \mid S_2^z S_3^z \ldots S_{2m-1}^z S_{2m}^z S_1^z \rangle \langle S_1^z S_2^z S_3^z \ldots S_{2m}^z \mid . \tag{10}$$

In the absence of magnetic field, the numerical calculations can be performed using the pure $S = 1/2$ isotropic Heisenberg model:

$$\mathcal{H} = -J \sum_{i=1}^{L} \mathbf{S}_i \mathbf{S}_{i+1}. \tag{11}$$

To confirm the reliability of the model (11), the QTM numerical results are compared with the Bethe ansatz (BA) results [18] which is an exact method and

then to establish the value of the exchange coupling J, the simulation results are compared with the experimental specific heat data for Yb_4As_3 compound [9]. The values of others parameters in Hamiltonian (3) are estimated from comparision with field-dependent specific heat experimental results of Yb_4As_3 [9].

In the presence of the external magnetic field applied perpendicular to the spin-chain in the model (3), the system is nonuniform because of induced staggered field, so we need define the partition function accordingly. Then the m-th approximant $\mathcal{Z}_m$ of the partition function $\mathcal{Z}$ is related to the two global transfer matrix $\mathcal{W}_1$ and $\mathcal{W}_2$:

$$Z_m = Tr\left(\mathcal{W}_1\mathcal{W}_2\right)^{L/2}, \text{ where } \mathcal{W}_1 = \left(\mathcal{P}^2\mathcal{L}_{1,2}\right)^m, \mathcal{W}_2 = \left(\mathcal{P}^2\mathcal{L}_{2,3}\right)^m \tag{12}$$

To calculate the partition function for finite chains we need to define two vectors which act in a Hilbert space $\mathcal{H}^{2m}$ [11,17,19]:

$$\mid a\rangle = \sum_{\{S^z\}} \prod_{r=1}^{2m} \delta_{S^z_{2r-1},S^z_{2r}} \mid S^z_1 \ldots S^z_{2m}\rangle\,, \tag{13}$$

$$\mid b\rangle = \sum_{\{S^z\}} \prod_{r=1}^{2m} \delta_{S^z_{2r},S^z_{2r+1}} \mid S^z_1 \ldots S^z_{2m}\rangle\,. \tag{14}$$

Then the m-th approximant of the partition function is different for odd and even number of sites in the chains:

$$\mathcal{Z}_m = \langle b \mid \left(\mathcal{W}_1\mathcal{W}_2\right)^{(L-1)/2} \mid a\rangle \quad \text{for} \quad \text{odd} \quad L\,, \tag{15}$$

$$\mathcal{Z}_m = \langle b \mid \left(\mathcal{W}_1\mathcal{W}_2\right)^{L/2} \mid a\rangle \quad \text{for} \quad \text{even} \quad L\,. \tag{16}$$

Taking the quantum limit $m \to \infty$ in (12), the partition function $\mathcal{Z}$ can be estimated and the corresponding thermodynamic function can be calculated. In order to improve the accuracy of the extrapolation for low temperatures, we have calculated the specific heat using the extrapolation polynomial of the degree k ($k = 1, \ldots, k_{max}$) in $1/m^2$.

$$C_k\left(\frac{1}{m^2}\right) = \sum_{j=0}^{k} a_j \cdot \left(\frac{1}{m^2}\right)^j. \tag{17}$$

The approximants C_m correspond to $m_{min} \leq m \leq m_{max}$. For practical reasons, in our procedure $k_{max} \leq 10$. The value of the highest Trotter index m_{max} is fixed and amounts to 14 or 15 in low temperatures and 13 in high temperatures. The value m_{min} is subject to variation in the region $2 \leq m_{min} \leq m_{max} - 1$.

The extrapolation procedure starts with $m_{min} = 2$ and is continued till $m = m_{max} - 1$. In each step the number of fitted points n ($n = m_{max} - m_{min} + 1$) is fixed and the extrapolations are performed with polynomials of the degree k ($1 \leq k \leq n - 1$, but not more than 10). In this way for a given field and

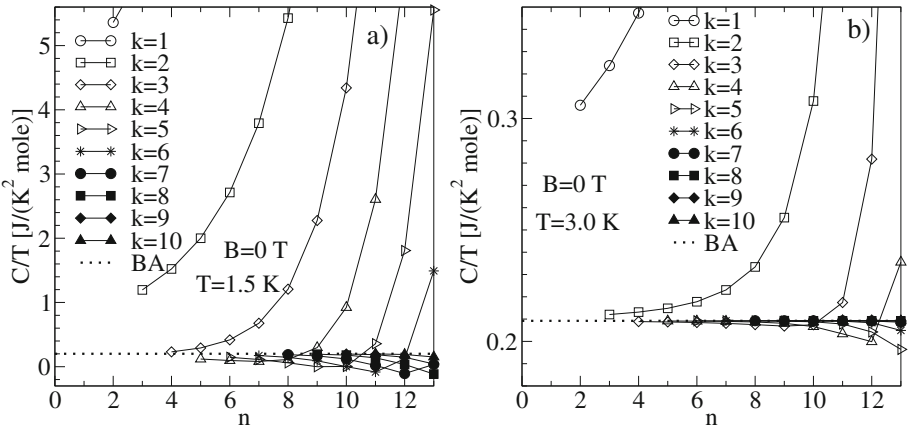

Fig. 1. The extrapolated values of specific heat versus the number of points n for which the polynomials are constructed. Each particular plot corresponds to the polynomial of a given degree k. The figures (a) and (b) have been drawn for infinite chains and $B = 0$ T with $T = 1.5$ K and $T = 3$ K, respectively. The QTM results are presented by symbols in reference to the Bethe ansatz results (dotted line).

temperature we obtain a set of extrapolated values for different values of n and k and we can present the variation of the data with n for the fixed degree k of the polynomial.

The results of the analysis of the extrapolated specific heat values according to the above procedure are shown in Fig. 1. To check the accuracy of the extrapolations performed for infinite chains, the plots were referred to the value obtained on the basis of the Bethe ansatz approach [18] which is shown as a dotted line in Fig. 1. As demonstrated, the convergence depends significantly on the degree k of the polynomial. The convergence of the extrapolated values is much better for higher temperatures and implies higher accuracy of the numerical estimates.

To describe the magnetic specific heat of diluted $(Yb_{1-x}Lu_x)_4As_3$ we need to calculate the contribution C_L of a finite chain with L sites and to find the probability distribution. Assuming the uniform distribution of non–magnetic Lu–ions among the chains, each site in the Yb^{3+}–chain is randomly occupied by a magnetic ion with a probability $p = 1 - x$. The probability of finding a chain with L sites is $p^L(1-p)^2$. The number of L–chains is $n_L = Np^L(1-p)^2$ ($N \to \infty$ is the total chain length and is much larger than the cluster length) and the total number of all L-chains is given by the following sum:

$$n_t = \sum_{L=1}^{\infty} n_L = N \sum_{L=1}^{\infty} p^L(1-p)^2 = N(1-p)^2 \sum_{L=1}^{\infty} p^L = N(1-p)p. \qquad (18)$$

Finally, we obtain the specific heat per spin:

$$C = x \sum_{L=1}^{\infty} \omega_L C_L, \tag{19}$$

where the probability distribution of chains with L sites [20]:

$$\omega_L = p^{L-1}(1-p). \tag{20}$$

For each temperature we have calculated within the QTM technique the specific heat $C(L)$ for $L \leq 30$. Our specific heat results for two temperatures ($T = 7$ and $T = 14$ K) and two configurations of magnetic field are shown in Fig. 2. The open symbols represent the specific heat for various numbers of sites L. The filled symbols represent specific heat data whose we have obtained using QTM technique for infinite chains. Those results are consistent with exact Bethe ansatz results [18]. For sufficiently large $L > L_0$ we can estimate the specific heat by the linear function and finally, specific heat for whole range of L [21]:

$$C = x^2 \cdot \sum_{L=1}^{L_0} (1-x)^L \cdot C(L)L + C(L > L_0). \tag{21}$$

We emphasize that the value L_0 exceeds the sizes where the domain of the exact diagonalization technique is applicable [21,22]. Moreover, the computational complexity of the QTM estimates C_L increases lineary with L which is additional advantage with respect to other techniques [14].

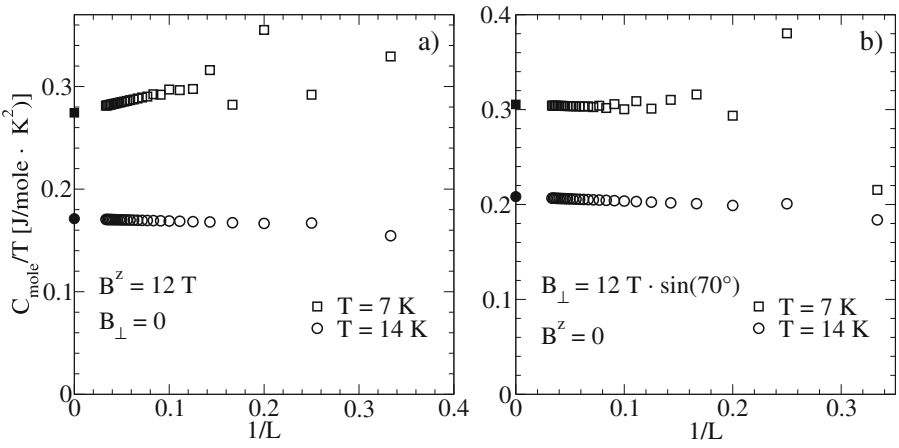

Fig. 2. Size dependence of specific heat calculated for finite segments with different number of sites L (open symbols). The filled symbols are the simulation results corresponding to the infinite chains. The external magnetic field is applied along the spin chain (a) and perpendicular to the spin chain (b).

3 The Results of the Numerical Simulations and Discussion

The QTM method described has been tested with respect to convergence in the Trotter index m and the size L, and has been applied to simulation via the Heisenberg model (3) of the experimental field-dependent specific heat data for diluted $(Yb_{1-x}Lu_x)_4As_3$ system of particular interest [5]. In order to calculate magnetic specific heat we assumed that 25% of the domains in the polydomain single cristal sample were oriented in parallel and 75% were oriented perpendicular to the direction of the applied field. The effective magnetic field $B_{eff} = B\sin(70°)$ is assumed to be oriented in the direction perpendicular to the chain [5]. Finally, the numerical specific heat result is given by:

$$C(T,B) = 0.75 \cdot C_{\perp}(T, B_{eff}) + 0.25 \cdot C_{\parallel}(T,B)\,. \tag{22}$$

The results of simulations and experimental data are shown in the Fig. 3 for the concentration of impurities $x = 3\%$ and for two different values of magnetic field $B = 6$ T and $B = 15$ T. The experimental data supplement those published before [5] and were measured using the same protocol.

As demonstrated in Fig. 3, the reliability of the simulation method and the model applied have been strongly verified. The simulations require the HPC recourses as far as the temporal and memory complexity are concerned. They can be efficiently parallelized [17,23–25] as the traces in (7) and (12) refer to

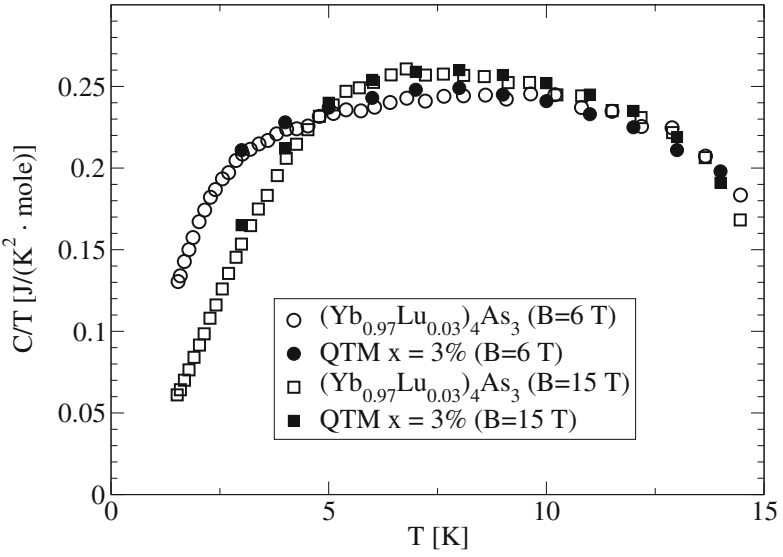

Fig. 3. Comparision between experiment and numerical results for the diluted samples subject to an applied field. The field applied is $B = 6$ T and 15 T. The concentration of nonmagnetic impurities $x = 3\%$.

the independent vectors in the Hilbert space. The finite size contributions C_L, depending on temperature and field, can be also evaluated for each L separately, i.e. in parallel.

In conclusion, we have presented the numerical QTM approach to characterize the finite temperature magnetic properties of the diluted $(Yb_{1-x}Lu_x)_4As_3$ system. We have successfully compared the results of our QTM simulations with the experimental findings. We have enhanced evidence that the spin model worked out for the pure compound Yb_4As_3 can also explain the specific heat results for the diluted systems, using their random distribution.

Acknowledgement. We thank for an access to the HPC resources in PSNC Poznań (Poland).

References

1. Köppen, M., Lang, M., Helfrich, R., Steglich, F., Thalmeier, P., Schmidt, B., Wand, B., Pankert, D., Benner, H., Aoki, H., Ochiai, A.: Phys. Rev. Lett. **82**, 4548 (1999)
2. Kohgi, M., Iwasa, K., Mignot, J.-M., Ochiai, A., Suzuki, T.: Phys. Rev. B **56**, R11388 (1997)
3. Schmidt, B., Aoki, H., Cichorek, T., Custers, J., Gegenwart, P., Kohgi, M., Lang, M., Langhammer, C., Ochiai, A., Paschen, S., Steglich, F., Suzuki, T., Thalmeier, P., Wand, B., Yaresko, A.: Phys. B **300**, 121 (2001)
4. Kohgi, M., Iwasa, K., Mignot, J.-M., Fak, B., Gegenwart, P., Lang, M., Ochiai, A., Aoki, H., Suzuki, T.: Phys. Rev. Lett. **86**, 2439 (2001)
5. Kamieniarz, G., Matysiak, R., Gegenwart, P., Ochiai, A., Steglich, F.: Phys. Rev. B **94**, 100403(R) (2016)
6. Oshikawa, M., Ueda, K., Aoki, H., Ochiai, A., Kohgi, M.: J. Phys. Soc. Jpn. **68**, 3181 (1999)
7. Shiba, H., Ueda, K., Sakai, O.: J. Phys. Soc. Jpn. **69**, 1493 (2000)
8. Shibata, N., Ueda, K.: J. Phys. Soc. Jpn. **70**, 3690 (2001)
9. Matysiak, R., Kamieniarz, G., Gegenwart, P., Ochiai, A.: Phys. Rev. B **79**, 224413 (2009)
10. Iwasa, K., Kohgi, M., Gukasov, A., Mignot, J.-M., Shibata, N., Ochiai, A., Aoki, H., Suzuki, T.: Phys. Rev. B **65**, 052408 (2002)
11. Delica, T., Leschke, H.: Phys. A **168**, 736 (1990)
12. Kamieniarz, G., Bieliński, M., Renard, J.-P.: Phys Rev. B **60**, 14521 (1999)
13. Kamieniarz, G., Matysiak, R., D'Auria, A.C., Esposito, F., Esposito, U.: Phys. Rev. B **56**, 645 (1997)
14. D'Auria, A.C., Esposito, U., Esposito, F., Gatteschi, D., Kamieniarz, G., Wałcerz, S.: J. Chem. Phys. **109**, 1613 (1998)
15. Barasiński, A., Kamieniarz, G., Drzewiński, A.: Comput. Phys. Commun. **182**, 2013 (2011)
16. Barasiński, A., Kamieniarz, G., Drzewiński, A.: Phys. Rev. B **86**, 214412 (2012)
17. Kamieniarz, G., Matysiak, R.: Comput. Mater. Sci. **28**, 353 (2003)
18. Johnston, D.C., Kremer, R.K., Troyer, M., Wang, X., Klümper, A., Bud'ko, S.L., Panchula, A.F., Canfield, P.C.: Phys. Rev. B **61**, 9558 (2000)
19. Kamieniarz, G., Matysiak, R.: J. Comput. Appl. Math. **189**, 471 (2006)
20. Asakawa, H., Matsuda, M., Minami, K., Yamazaki, H., Katsumata, K.: Phys. Rev. B **57**, 8285 (1998)

21. Matysiak, R., Gegenwart, P., Ochiai, A., Antkowiak, M., Kamieniarz, G., Steglich, F.: Phys. Rev. B **88**, 224414 (2013)
22. Kamieniarz, G., Matysiak, R., D'Auria, A.C., Esposito, F., Benelli, C.: Eur. Phys. J. B **23**, 183 (2001)
23. Kamieniarz, G., Matysiak, R., D'Auria, A.C., Esposito, F., Benelli, C.: Application of parallel computing in the transfer — matrix simulations of the supramolecules Mn_6 and Ni_12. In: Wyrzykowski, R., Dongarra, J., Paprzycki, M., Waśniewski, J. (eds.) PPAM 2001. LNCS, vol. 2328, pp. 502–509. Springer, Heidelberg (2002). https://doi.org/10.1007/3-540-48086-2_55
24. Kamieniarz, G., Matysiak, R.: Deterministic large-scale simulations of the low-dimensional magnetic spin systems. In: Wyrzykowski, R., Dongarra, J., Paprzycki, M., Waśniewski, J. (eds.) PPAM 2003. LNCS, vol. 3019, pp. 1091–1098. Springer, Heidelberg (2004). https://doi.org/10.1007/978-3-540-24669-5_141
25. Antkowiak, M., Kucharski, Ł., Matysiak, R., Kamieniarz, G.: Comput. Methods Sci. Technol. **22**, 87 (2016)